An Online Radio Map Update Scheme for WiFi Fingerprint-Based Localization

Baoqi Huang, *Member, IEEE*, Zhendong Xu, Bing Jia, *Member, IEEE*, and Guoqiang Mao, *Fellow, IEEE*

***Abstract*—Fingerprint-based localization relies on an accurate and up-to-date radio map, which is however cumbersome to obtain. In this paper, a novel scheme is proposed to online adapt radio maps to environmental dynamics by using low-cost crowdsourced received signal strength (RSS) measurements. To be specific, a coarse-grained radio map is initially established in the offline phase utilizing the standard Gaussian process regression (GPR) given a limited number of fingerprints (i.e., RSS measurements with location labels), and further can be recursively refined in the online phase given crowdsourced RSS measurements with their noisy location labels obtained through the existing radio map. Differently from existing GPR-based approaches, the proposed scheme adopts extended GPR to alleviate the model inaccuracy induced by such noisy location labels, and then presents a marginalized particle extended Gaussian process (MPEG) to recursively filter the radio map. In addition, pedestrian dead reckoning (PDR) is leveraged to calibrate such noisy location labels. Extensive experiments are carried out in a real scenario with area of nearly 1000 m^2 during a five-month period of time, and a thorough comparison with several existing approaches indicates that the proposed scheme gradually improves the localization accuracy on average by as much as 31.2%, while the counterparts result in fluctuant localization performance and improve the localization accuracy on average by 13.3%.**

***Index Terms*—Crowdsourcing, fingerprinting, indoor localization, radio map.**

I. Introduction

THE explosive proliferation of mobile devices have spurred extensive demands on location-based services (LBSs) in recent decades. The global positioning system (GPS) has been widely used in outdoor positioning, but cannot work in indoor environments due to a lack of line of sight (LoS) transmission channels between satellites and indoor receivers [1]. Therefore, in the past two decades great efforts have been devoted to developing indoor positioning systems (IPSs) to enable reliable and precise indoor positioning and navigation [2], [3]. Nowadays, WiFi network infrastructures are available in almost every commercial and residential building, and nearly every off-the-shelf mobile device supports WiFi. As such, WiFi-based localization, especially the WiFi fingerprint-based method [4]–[8], has become an attractive alternative to GPS in indoor environments.

Basically, a fingerprint essentially comprises of a vector of statistical attributes (e.g., mean, variance, and histogram) of or simply received signal strength (RSS) measurements from multiple APs and the location labels attached to the RSS measurements [4]. The fingerprint-based method normally involves the following two major steps [8]. In the first step, a radio map consisting of a number of fingerprints collected at specific locations is constructed via an offline site survey. In the second step, when a device sends an online location query containing the current vector of RSS measurements, its location is estimated according to the current radio map.

Building a radio map demands labor-intensive and time-consuming measurement campaigns in an offline site survey, imposing a severe limitation on implementing fingerprint-based IPSs. Hence, it is of great importance to reduce the workload in building radio maps. To that end, a number of approaches have been reported. For instance, the crowdsourcing-based approaches [9]–[14] leverage daily activities of participants to automatically collect fingerprints so as to save manpower. Recently, the Gaussian process regression (GPR)-based approaches [15], [16] gained much attention since the number of RSS measurements is substantially reduced.

Apart from the difficulties in efficiently building radio maps, the localization performance of fingerprint-based IPSs often degrades over time due to environmental dynamics which lead to the discrepancy between the current signal features and the historically established radio map. As such, significant research [17]–[23] has been conducted to produce update-to-date radio maps. However, existing studies are still confronted with the following issues. First, the location labels attached to crowdsourced RSS measurements normally incur uncertainties, which result in model inaccuracy, but most studies [20] simply ignore this issue when updating radio maps and thus suffer from robustness. Second, different approaches may impose various restrictions, like using dedicated devices [21], [22], performing specific activities [23], and producing intractable radio maps [19]. Last but not least, the existing GPR-based approaches [15], [16], [20], [22] have limited scalability because it is usually time-consuming and

Manuscript received January 21, 2019; revised April 9, 2019; accepted April 18, 2019. Date of publication April 23, 2019; date of current version July 31, 2019. This work was supported in part by the National Natural Science Foundation of China under Grant 41871363, Grant 41761086, Grant 61461037, and Grant 61761035, in part by the Natural Science Foundation of Inner Mongolia Autonomous Region of China under Grant 2017JQ09, and in part by the "Grassland Elite" Project of the Inner Mongolia Autonomous Region under Grant CYYC5016. *(Corresponding author: Bing Jia.)*

B. Huang, Z. Xu, and B. Jia are with the College of Computer Science, Inner Mongolia University, Hohhot 010021, China (e-mail: jiabing@imu.edu.cn).

G. Mao is with the School of Computing and Communication, University of Technology Sydney, Ultimo, NSW 2007, Australia, and also with Data61, CSIRO, Canberra, ACT 2601, Australia.

Digital Object Identifier 10.1109/JIOT.2019.2912808

error-prone to invert the associated covariance matrix given a huge amount of crowdsourced fingerprints.

To address the above issues, this paper proposes a systematic scheme to generate and recursively update a radio map by exploiting crowdsourced fingerprints. Specifically, during the offline site survey, a coarse-grained radio map associated with a set of predefined locations (e.g., the points on a regular lattice) is initially built using the standard GPR given a limited number of fingerprints, which can be rapidly derived by traversing the target space with their location labels obtained through, e.g., manual configuration; then, during the online localization, this radio map is recursively refined by making use of fingerprints crowdsourced at arbitrary locations which can be obtained through the currently available radio map. As such, it is unnecessary to align the location labels of crowdsourced fingerprints with the predefined locations. Moreover, the proposed scheme leverages pedestrian dead reckoning (PDR) [24] to calibrate the noisy location labels as well as the extended GPR [25] to alleviate the model inaccuracy, which enhances the performance and robustness of the radio map. On these grounds, a marginalized particle extended Gaussian process (MPEG) is presented based on the framework in [26] to recursively filter the radio map given newly crowdsourced fingerprints, so that filtering with a huge amount of crowdsourced fingerprints can be implemented in an online divide and conquer manner. Extensive experiments are carried out in a real scenario with the area of nearly 1000 m^2 during five months. A thorough comparison with the original fingerprint-based IPS and other popular approaches confirms the feasibility and validity of the proposed scheme, and indicates that the proposed scheme is able to gradually improve the localization accuracy, while the counterparts result in fluctuant and low localization performance.

The rest of this paper is organized as follows. Section II reviews the literature. Section III provides an overview of the proposed scheme. Section IV extends the standard GPR to mitigate the influence of noisy location labels and further adopts PDR to calibrate noisy location labels. Section V presents the design and implementation of MPEG in detail. In Section VI, experimental results and performance evaluation are reported. We conclude this paper in Section VII.

II. Related Works

In this section, we shall briefly review the literature on generating and updating radio maps, respectively.

Since fingerprint is usually represented by either the statistical attributes or the distribution of corresponding RSS measurements, the more are the RSS measurements, the better is the resulting radio map, but the site survey cost also becomes higher. Therefore, existing studies mainly focus on balancing the efforts spent and the resulting localization performance, and can be categorized into the model-based approach, crowdsourcing-based approach, and optimization-based approach. The model-based approach uses various WiFi signal propagation models to predict RSS measurements at different locations instead of measurement campaigns [27]. However, none of models can accurately characterize signal propagations in complicated indoor environments. The crowdsourcing-based approach leverages undedicated daily activities to collect RSS measurements, and in combination with other localization techniques like PDR, to provide crowdsourced fingerprints. In [9], a novel technique is proposed based on the Gaussian process latent variable model (GPLVM) to determine the latent-space locations of unlabeled RSS measurements. In [10]–[12], PDR and extra environmental information, e.g., virtual landmarks, floor layout, etc., was exploited to infer the location labels of crowdsourced fingerprints. The optimization-based approach estimates radio maps using only a limited number of fingerprints. In [13], a hybrid generative/discriminative semi-supervised learning algorithm was proposed to utilize a large number of unlabeled RSS measurements to supplement a small number of fingerprints. In [28], an unsupervised manifold alignment was used to estimate radio maps given only 1% of the fingerprinting load, some crowdsourced RSS measurements and an indoor map. In [15] and [16], the spatial correlation between nearby fingerprints is employed to interpolate or calibrate radio maps.

Furthermore, different types of attempts have been made to adapt existing radio maps to environmental dynamics. One kind of solutions only consider the changes of APs and replaces the outdated fingerprints in radio maps [17], [18]. Another kind of solutions try to fuse new fingerprints with existing radio maps. In [19], LuMA modeled the problem of updating a radio map as a transfer learning problem based on dimensionality reduction, which learns a mapping from an old radio map to a new one in a low-dimensional space. In [20], a dynamic online-calibration scheme was proposed to apply the GPR with the log-distance path loss model to construct and calibrate radio maps, but required re-estimating the parameters by maximizing the given likelihood function. Recently, a WiFi-based nonintrusive IPS was proposed in [21] by using RSS measurements between APs to online calibrate radio maps. Similar scheme was reported in [22] by placing dedicated devices at fixed locations. Additionally, in [23], AcMu makes use of realtime RSS measurements from a static smartphone to automatically update radio maps by modeling the underlying relationship between nearby RSS measurements, which relies on the movement detection of the smartphone.

To sum up, we can conclude that: 1) intensive efforts have been invested on generating radio maps using crowdsourced RSS measurements in the offline phase; 2) the studies on radio map update in the online phase by fusing fresh RSS measurements with existing radio maps is relatively limited; and 3) the uncertainties in locations labels are ignored. Unlike the existing studies that separately tackle the problems in the offline and online phases, this paper presents an approach that seamlessly combines the generation and update of radio maps, so as to improve its robustness and scalability.

III. Overview of the Scheme

The proposed scheme is similar to most traditional fingerprint-based IPSs except that the standard GPR, PDR, and MPEG are introduced, as illustrated in Fig. 1.

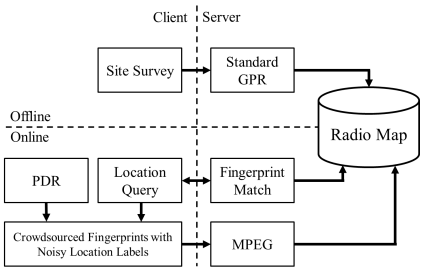

Fig. 1. System architecture of the proposed scheme.

In the offline phase, a lightweight site survey is initially conducted to collect a limited number of fingerprints. Specifically, a smartphone user is asked to traverse the target space at a constant speed to collect RSS measurements from nearby APs, and meanwhile, the coordinates and times associated with the beginning position and ending position of every straight path are recorded to further infer the location labels. After that, a coarse-grained radio map associated with a set of predefined locations in the target space, e.g., the positions on a regular lattice, can be produced based on the standard GPR which is able to sufficiently make use of the spatial correlations among the limited number of fingerprints.

In the online phase, as long as a location query including current RSS measurements is sent to the server, a fingerprint matching algorithm, e.g., k nearest neighbor (KNN), will be executed to determine and return a most possible location according to the radio map. Differently from traditional fingerprint-based IPSs, the proposed scheme leverages participants to crowdsource fingerprints in the online phase. Particularly, a set of RSS measurements from nearby APs is derived when a participant traverses the target space, and is sent to the server together with their initial location estimates determined based on the current fingerprint-based IPS and PDR information (i.e., step count, step length, and heading); then, the server will run MPEG to update the radio map in an online fashion by using these crowdsourced fingerprints.

In summary, the proposed scheme can be readily integrated into an existing fingerprint-based IPS, so as to recursively adapt its radio map to realtime environments using crowdsourced fingerprints. Even though the location labels of crowdsourced fingerprints are often different, only the fingerprints at the predefined locations are maintained, and the size of the radio map does not change over time.

IV. Processing Noisy Location Labels

In this section, we first briefly introduce the preliminaries on the standard GPR from the perspective of fingerprint-based localization, then present how to extend the GPR to train a radio map using RSS measurements with noisy location labels, and finally calibrate noisy location labels based on PDR.

Throughout this paper, letters in bold denote matrix or vector; $\mathbb{E}(\cdot)$, $\mathbb{V}(\cdot)$, and $\mathbb{C}(\cdot,\cdot)$ denote the expectation, variance, and covariance operators, respectively; $\|\cdot\|$ denotes the Euclidean norm operator; superscript T denotes the transpose operator; and $\mathbf{I}$ is the identity matrix.

A. Standard GPR

For ease of presentation, we only consider one WiFi AP. At first, let y denote an RSS measurement in dBm collected at a particular location with precise coordinates $\mathbf{x} \in \mathbb{R}^2$ from this AP. Then, by regarding the RSS measurement y as the observation and the coordinates $\mathbf{x}$ as the input feature, we can have the following observation model:

$$y = f(\mathbf{x}) + \varepsilon \tag{1}$$

where $f(\mathbf{x})$ maps the input, i.e., the location coordinates $\mathbf{x}$, to a Gaussian random variable $\sim \mathcal{N}(m(\mathbf{x}), \sigma_f^2)$, and ε denotes the observation noise and satisfies $\mathcal{N}(0, \sigma^2)$. Since the accurate form of $m(\mathbf{x})$ is difficult to derive, the following quadratic polynomial function of $\mathbf{x}$ is employed according to [16]:

$$m(\mathbf{x}) = \mathbf{x}^{\mathrm{T}}\mathbf{A}\mathbf{x} + \mathbf{b}^{\mathrm{T}}\mathbf{x} + c \tag{2}$$

where $\mathbf{A} = \mathbf{A}^{\mathrm{T}}$, $\mathbf{A} \in \mathbb{R}^{2\times 2}$, $\mathbf{b} \in \mathbb{R}^2$, and $c \in \mathbb{R}$.

Then, given n coordinates $\mathbf{X} = [\mathbf{x}_1 \ \ldots \ \mathbf{x}_n]$, the vector of $f(\mathbf{x})$, denoted $\mathbf{f}(\mathbf{X})$, is multivariate Gaussian with the mean vector function $\mathbf{m}(\mathbf{X}) = [m(\mathbf{x}_1), \ldots, m(\mathbf{x}_n)]^{\mathrm{T}}$, and the covariance matrix function $\mathbf{K}(\mathbf{X}, \mathbf{X})$, namely, that $\mathbf{f}(\mathbf{X})$ is a Gaussian process (GP). The element on the ith row and jth column of $\mathbf{K}(\mathbf{X}, \mathbf{X}')$ can be modeled by using the commonly adopted squared exponential kernel function [9] as follows:

$$k\left(\mathbf{x}_i, \mathbf{x}'_j\right) = \sigma_f^2 \exp\left(-\frac{\|\mathbf{x}_i - \mathbf{x}'_j\|}{2l^2}\right) \tag{3}$$

where $\mathbf{x}_i, \mathbf{x}'_j$ denote the ith column of $\mathbf{X}$ and jth column of $\mathbf{X}'$, respectively; l denotes the scale parameter.

As such, the corresponding RSS measurements, i.e., $\mathbf{y} = [y_1, \ldots, y_n]^{\mathrm{T}}$, satisfy

$$\mathbf{y}|\mathbf{X} \sim \mathcal{N}\left(\mathbf{m}(\mathbf{X}), \mathbf{K}(\mathbf{X}, \mathbf{X}) + \sigma^2\mathbf{I}\right) \tag{4}$$

where $\mathbf{I}$ has the order of n.

B. Extended GPR

As mentioned above, the coordinates $\mathbf{x}$ and $\mathbf{X}$ are assumed to be exactly known, which can be satisfied in the traditional approach by cumbersomely and manually measuring the required coordinates, whereas in our case, the location labels of crowdsourced RSS measurements are often derived through certain estimation approaches (e.g., WiFi fingerprint-based IPS and PDR) and inevitably suffer from noises. Therefore, instead of the true coordinates (i.e., $\mathbf{x}$), the observed location label (i.e., $\mathbf{u}$) corrupted by noises (i.e., $\boldsymbol{\eta}$) has to be employed to approximately formulate the GPR model, as depicted in Fig. 2, which certainly leads to model inaccuracy and thus degrades the performance to some extent.

In order to improve the performance of radio maps built through the GPR approach, it is necessary to adopt the approach in [25] to extend the standard GPR to accommodate the uncertainties in the location labels. To this end, given the noisy location label $\mathbf{u}$, we can establish the following model:

$$\mathbf{u} = \mathbf{x} + \boldsymbol{\eta} \tag{5}$$

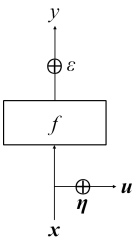

Fig. 2. GPR and its input being observed with noises.

where the uncertainty $\boldsymbol{\eta}$ is assumed to be white Gaussian with the covariance matrix $\mathbb{V}(\boldsymbol{\eta})$.

It follows from (1) and (5) that $y = f(\mathbf{u} - \boldsymbol{\eta}) + \varepsilon$, and by applying the first order Taylor expansion around $\mathbf{u}$, we have:

$$y \approx f(\mathbf{u}) - \boldsymbol{\eta}^{\mathrm{T}} \frac{\partial f}{\partial \mathbf{u}} + \varepsilon. \tag{6}$$

Then, the derivative of the random function $f(\mathbf{u})$ can be approximated by the derivative of its mean function $m(\mathbf{u})$, denoted by $\boldsymbol{\partial}_{\bar{f}(\mathbf{u})}$, and then we can have

$$y \approx f(\mathbf{u}) - \boldsymbol{\eta}^{\mathrm{T}} \boldsymbol{\partial}_{\bar{f}(\mathbf{u})} + \varepsilon \tag{7}$$

which provides an approximate model describing the relationship between the RSS measurement y and the random variable $f(\cdot)$ with noisy location labels. Assuming the independence between $\boldsymbol{\eta}$ and ε, we can obtain the following distributions:

$$y|f(\mathbf{u}) \sim \mathcal{N}\Big(f(\mathbf{u}), \boldsymbol{\partial}^{\mathrm{T}}_{\bar{f}(\mathbf{u})} \mathbb{V}(\mathbf{u}) \boldsymbol{\partial}_{\bar{f}(\mathbf{u})} + \sigma^2\Big). \tag{8}$$

Given the n noisy location labels $\mathbf{U} = [\mathbf{u}_1, \ldots, \mathbf{u}_n]$ with the ground truth $\mathbf{X}$ and in combination with the distribution of $\mathbf{f}(\mathbf{U})$, we can have

$$\mathbf{y}|\mathbf{U} \sim \mathcal{N}(\mathbf{m}(\mathbf{U}), \mathbf{Q}(\mathbf{U})) \tag{9}$$

where

$$\mathbf{Q}(\mathbf{U}) = \mathbf{K}(\mathbf{U}, \mathbf{U}) + \boldsymbol{\partial}^{\mathrm{T}}_{\bar{\mathbf{f}}(\mathbf{U})} \Sigma_{\mathbf{U}} \boldsymbol{\partial}_{\bar{\mathbf{f}}(\mathbf{U})} + \sigma^2 \mathbf{I} \tag{10}$$

with $\boldsymbol{\partial}_{\bar{\mathbf{f}}(\mathbf{U})} = \mathrm{diag}[\boldsymbol{\partial}_{\bar{f}(\mathbf{u}_1)}, \ldots, \boldsymbol{\partial}_{\bar{f}(\mathbf{u}_n)}]$ and $\Sigma_{\mathbf{U}} = \mathbb{C}(\mathbf{U}, \mathbf{U})$.

Let $\mathbf{A}, \mathbf{b}, c, \sigma, \sigma_f, l$ be the hyperparameters of the GP, denoted $\boldsymbol{\theta}$. Given a set of crowdsourced fingerprints, i.e., RSS measurements $\mathbf{y}$ and noisy location labels $\mathbf{U}$, the maximum likelihood estimator (MLE) can be utilized based on (9) to estimate $\boldsymbol{\theta}$, so that the mean and variance of RSS measurements at any location, say $\mathbf{x}_*$, can be predicted as follows:

$$\begin{aligned}\mathbb{E}(f_*|\mathbf{U}, \mathbf{y}, \mathbf{x}_*) &= m(\mathbf{x}_*) \\ &\quad + \mathbf{K}(\mathbf{x}_*, \mathbf{U})^{\mathrm{T}} \mathbf{Q}(\mathbf{U})^{-1} (\mathbf{y} - \mathbf{m}(\mathbf{U}))\end{aligned} \tag{11}$$

$$\begin{aligned}\mathbb{V}(f_*|\mathbf{U}, \mathbf{y}, \mathbf{x}_*) &= k(\mathbf{x}_*, \mathbf{x}_*) \\ &\quad - \mathbf{K}(\mathbf{x}_*, \mathbf{U})^{\mathrm{T}} \mathbf{Q}(\mathbf{U})^{-1} \mathbf{K}(\mathbf{x}_*, \mathbf{U})\end{aligned} \tag{12}$$

where the functions $m(\cdot)$, $k(\cdot, \cdot)$, $\mathbf{K}(\cdot, \cdot)$, and $\mathbf{Q}(\cdot)$ are evaluated by using the estimates of the hyperparameters.

Regarding each AP, its specific hyperparameters can be estimated, such that the mean and variance of RSS measurements at the predefined locations from this AP can be evaluated through (11) and (12) for generating the corresponding radio map. Since the new model (9), provides a more accurate characterization as to crowdsourced fingerprints, it is promising that more accurate means and variances can be obtained in comparison with the standard GPR, and thus more accurate radio maps can be derived.

C. Calibrating Location Labels

In order to further improve the accuracy of radio maps, PDR is introduced to calibrate the location labels attached to crowdsourced RSS measurements. The basic idea is to formulate a constrained optimization problem to fuse the initial location estimates returned by using the current radio map and PDR information in relation to a trajectory traversed by any crowdsourcing participant.

Prior to fusing such two sources of information, we have to align them in the time domain because the frequency of WiFi scan for collecting RSS measurements is usually not synchronized with the step frequency of PDR. Without loss of generality, suppose the frequency of WiFi scan is 1 Hz; instead of directly using steps, the progress that a crowdsourcing participant can make during 1 s, denoted d m, is thus employed to realize the alignment. It is noticeable that d can be easily inferred by using the corresponding step length and step frequency involved in PDR. Additionally, the heading estimate that is closest to the corresponding WiFi scan in the time domain is selected for use.

Given a trajectory delivering crowdsourced RSS measurements at j time instances, their initial locations, denoted by $[\mathbf{l}_1, \ldots, \mathbf{l}_j]$, can be estimated based on the fingerprint-based localization method using the existing radio map. Then, by letting $\mathbf{u}_1, \ldots, \mathbf{u}_j$ with $\mathbf{u}_i = [\,\mathbf{u}_i^x \;\; \mathbf{u}_i^y\,]$ denote the calibrated location labels, we can establish the following constrained least squares problem:

$$\begin{aligned}\min_{\mathbf{u}_1, \ldots, \mathbf{u}_j} \; & \sum_{i=1}^{j} \|\mathbf{u}_i - \mathbf{l}_i\|^2 \\ \text{s.t.} \; & \left|\mathbf{u}_i^x - \mathbf{u}_{i+1}^x\right| \le (d + \Delta d)\cos(\varphi_i \pm \Delta\varphi) \\ & \left|\mathbf{u}_i^y - \mathbf{u}_{i+1}^y\right| \le (d + \Delta d)\sin(\varphi_i \pm \Delta\varphi), \\ & \text{with } i = 1, 2, \ldots, j-1\end{aligned} \tag{13}$$

where φ_i denotes the heading estimate at time instance i, and Δd and $\Delta\varphi$ denote the upper bound on the distance error and heading error, which will be empirically set as 0.15 m and 0.15 radian, respectively, in the following experiments. Moreover, $\cos(\varphi_i \pm \Delta\varphi)$ (or $\sin(\varphi_i \pm \Delta\varphi)$) denotes the maximum value of $\cos(\varphi)$ (or $\sin(\varphi)$) with $\varphi \in [\varphi_i - \Delta\varphi, \varphi_i + \Delta\varphi]$. The heading and the step count can be estimated according to [29], and the step length according to [30].

V. Online Radio Map Update

According to Fig. 1, given a sufficient number of crowdsourced fingerprints, MPEG updates the current radio map based on the marginalized GPR framework in [26]. In what follows, we shall introduce the state space model in MPEG, then present the filtering process, and finally summarize MPEG. Similarly to the treatment in the previous section, we also take a single AP for example.

A. State Space Model

It is intuitive that building a radio map demands the expected RSS measurements at a set of predefined locations, which can be approximated by using (11). Hence, the state consists of the hyperparameters of the GP and the values of the GP at a given set of locations.

First, since there does not exist a rule guiding the hyperparameters to evolve with time, an artificial evolution using kernel smoothing which guarantees the estimation convergence [26], [31] is adopted, namely,

$$\boldsymbol{\theta}_t = b\boldsymbol{\theta}_{t-1} + (1-b)\bar{\boldsymbol{\theta}}_{t-1} + s_{t-1} \tag{14}$$

where b is a weight between 0 and 1, $\bar{\boldsymbol{\theta}}_{t-1}$ is the Monte Carlo mean of $\boldsymbol{\theta}$ at $t-1$, and $s_{t-1} \sim \mathcal{N}(0, r^2\Sigma_{t-1})$ with $r^2 = 1-b^2$ and Σ_{t-1} being the Monte Carlo variance matrix of $\boldsymbol{\theta}_{t-1}$.

Second, by exploiting the property of a multivariate Gaussian distribution that the GP $\mathbf{f}(\cdot)$ satisfies, a Kalman filter can be formulated to describe the iterative relationship of the GP. Specifically, define $\mathbf{U}_t^c = [\mathbf{U}_t, \mathbf{X}_*]$ and $\mathbf{f}_t^c = \mathbf{f}(\mathbf{U}_t^c)$, where $\mathbf{U}_t$ is the noisy location labels of the crowdsourced fingerprints at t and $\mathbf{X}_*$ contains the predefined locations for building the radio map. Since the prior distribution $p(\mathbf{f}_t^c, \mathbf{f}_{t-1}^c | \mathbf{U}_{t-1}^c, \mathbf{U}_t^c, \boldsymbol{\theta}_t)$ is jointly Gaussian, according to the conditional property of the multivariate Gaussian distribution [32], $p(\mathbf{f}_t^c | \mathbf{f}_{t-1}^c, \mathbf{U}_{t-1}^c, \mathbf{U}_t^c, \boldsymbol{\theta}_t)$ is Gaussian and satisfies

$$\mathcal{N}\big(\mathbf{G}(\boldsymbol{\theta}_t)\mathbf{f}_{t-1}^c + \mathbf{F}(\boldsymbol{\theta}_t), \mathbf{V}(\boldsymbol{\theta}_t)\big) \tag{15}$$

where

$$\mathbf{G}(\boldsymbol{\theta}_t) = \mathbf{K}_t\big(\mathbf{U}_t^c, \mathbf{U}_{t-1}^c\big)\mathbf{K}_t^{-1}\big(\mathbf{U}_{t-1}^c, \mathbf{U}_{t-1}^c\big) \tag{16}$$

$$\mathbf{F}(\boldsymbol{\theta}_t) = \mathbf{m}_t\big(\mathbf{U}_t^c\big) - \mathbf{G}(\boldsymbol{\theta}_t)\mathbf{m}_t\big(\mathbf{U}_{t-1}^c\big) \tag{17}$$

$$\mathbf{V}(\boldsymbol{\theta}_t) = \mathbf{K}_t\big(\mathbf{U}_t^c, \mathbf{U}_t^c\big) - \mathbf{G}(\boldsymbol{\theta}_t)\mathbf{K}_t\big(\mathbf{U}_t^c, \mathbf{U}_{t-1}^c\big)^{\mathrm{T}} \tag{18}$$

and the subscript of $\mathbf{K}_t$ and $\mathbf{m}_t$ means that the function is evaluated with respect to $\boldsymbol{\theta}_t$.

Hence, the following state equation can be derived by transforming the conditional density in (15) into a linear equation of the function value with noises $\mathbf{v}_t^f \sim \mathcal{N}(\mathbf{0}, \mathbf{V}(\boldsymbol{\theta}_t))$:

$$\mathbf{f}_t^c = \mathbf{G}(\boldsymbol{\theta}_t)\mathbf{f}_{t-1}^c + \mathbf{F}(\boldsymbol{\theta}_t) + \mathbf{v}_t^f. \tag{19}$$

Moreover, the observation equation could be directly obtained from the RSS measurements at t

$$\mathbf{y}_t = \mathbf{H}_t\mathbf{f}_t^c + \mathbf{v}_t^y \tag{20}$$

where $\mathbf{H}_t = [\mathbf{I}, \mathbf{0}]$ is an index matrix to make $\mathbf{H}_t\mathbf{f}_t^c = \mathbf{f}(\mathbf{U}_t)$, the order of $\mathbf{I}$ is n_t representing the number of noisy location labels in $\mathbf{U}_t$, and v_t^y is additive Gaussian noise satisfying $\mathcal{N}(\mathbf{0}, \boldsymbol{\partial}_{\bar{\mathbf{f}}(\mathbf{U}_t)}^{\mathrm{T}}\Sigma_{\mathbf{U}}\boldsymbol{\partial}_{\bar{\mathbf{f}}(\mathbf{U}_t)} + \sigma^2\mathbf{I})$ according to (8).

To sum up, the state space model is specified by (14), (19), and (20), and involves both nonlinear and linear parts, motivating us to adopt the marginalized particle filtering technique to resolve it.

B. Filtering With MPEG

We base MPEG on the recursive filtering framework proposed in [26] to simultaneously learn hyperparameters and estimate hidden function values at the predefined locations.

According to the state space model presented in the above section, we aim to the compute the posterior distribution $p(\mathbf{f}_t^c, \boldsymbol{\theta}_{1:t} | \mathbf{U}_{1:t}, \mathbf{X}_*, \mathbf{y}_{1:t})$, which can be factorized into two multiplicative terms based on the Bayes rule, i.e., $p(\boldsymbol{\theta}_{1:t} | \mathbf{U}_{1:t}, \mathbf{X}_*, \mathbf{y}_{1:t})$ and $p(\mathbf{f}_t^c | \boldsymbol{\theta}_{1:t}, \mathbf{U}_{1:t}, \mathbf{X}_*, \mathbf{y}_{1:t})$. Then, the first term can be factorized into the following recursive form:

$$\begin{aligned} p(\boldsymbol{\theta}_{1:t} | \mathbf{U}_{1:t}, \mathbf{X}_*, \mathbf{y}_{1:t}) &\propto p(\mathbf{y}_t | \mathbf{y}_{1:t-1}, \boldsymbol{\theta}_{1:t}, \mathbf{U}_{1:t}, \mathbf{X}_*) \\ &\quad \times p(\boldsymbol{\theta}_t | \boldsymbol{\theta}_{t-1}) p(\boldsymbol{\theta}_{1:t-1} | \mathbf{U}_{1:t-1}, \mathbf{X}_*, \mathbf{y}_{1:t-1}) \end{aligned} \tag{21}$$

which can be used to form a particle filter framework.

For each particle at time t, the hyperparameters $\boldsymbol{\theta}_t$ are drawn according to the proposal distribution $p(\boldsymbol{\theta}_t | \boldsymbol{\theta}_{t-1})$ [obtained from (14)], and the importance weight can be computed based on $p(\mathbf{y}_t | \mathbf{y}_{1:t-1}, \boldsymbol{\theta}_{1:t}, \mathbf{U}_{1:t}, \mathbf{X}_*)$, which can be solved analytically as follows:

$$\begin{aligned} &p(\mathbf{y}_t | \mathbf{y}_{1:t-1}, \boldsymbol{\theta}_{1:t}, \mathbf{U}_{1:t}, \mathbf{X}_*) \\ &= \int p\big(\mathbf{y}_t | \mathbf{f}_t^c, \boldsymbol{\theta}_t, \mathbf{U}_t, \mathbf{X}_*\big) p\big(\mathbf{f}_t^c | \mathbf{y}_{1:t-1}, \boldsymbol{\theta}_{1:t}, \mathbf{U}_{1:t}, \mathbf{X}_*\big)\, \mathrm{d}\,\mathbf{f}_t^c \\ &= \mathcal{N}\Big(\mathbf{H}_t\mathbf{f}_{t|t-1}^c, \mathbf{H}_t\mathbf{P}_{t|t-1}^c\mathbf{H}_t^{\mathrm{T}} + \boldsymbol{\partial}_{\bar{\mathbf{f}}(\mathbf{U}_t)}^{\mathrm{T}}\Sigma_{\mathbf{U}}\boldsymbol{\partial}_{\bar{\mathbf{f}}(\mathbf{U}_t)} + \sigma^2\mathbf{I}\Big) \end{aligned} \tag{22}$$

where $p(\mathbf{y}_t | \mathbf{f}_t^c, \boldsymbol{\theta}_t, \mathbf{U}_t, \mathbf{X}_*) \sim \mathcal{N}(\mathbf{H}_t\mathbf{f}_t^c, \boldsymbol{\partial}_{\bar{\mathbf{f}}(\mathbf{U}_t)}^{\mathrm{T}}\Sigma_{\mathbf{U}}\boldsymbol{\partial}_{\bar{\mathbf{f}}(\mathbf{U}_t)} + \sigma^2\mathbf{I})$ [refers to (20)], $p(\mathbf{f}_t^c | \mathbf{y}_{1:t-1}, \boldsymbol{\theta}_{1:t}, \mathbf{U}_{1:t}, \mathbf{X}_*) = \mathcal{N}(\mathbf{f}_{t|t-1}^c, \mathbf{P}_{t|t-1}^c)$ is the prediction step of Kalman filter for $\mathbf{f}_t^c$ which is also Gaussian distributed with the predictive mean $\mathbf{f}_{t|t-1}^c$ and covariance $\mathbf{P}_{t|t-1}^c$. After that, the second term associated with this particle can be filtered using Kalman filter since $\mathbf{f}_t^c$ is the hidden state in (19) and (20).

C. Algorithm

Putting everything together, we can summarize the whole algorithm as follows: at time $t = 1, 2, 3, \ldots$

1) For each particle, say the ith one for $i = 1, 2, \ldots, N$.
   a) Drawing hyperparameters $\boldsymbol{\theta}_t^i$ according to the proposal distribution $p(\boldsymbol{\theta}_t | \tilde{\boldsymbol{\theta}}_{t-1}^i)$.
   b) Calculating the parameters, e.g., $\mathbf{G}(\boldsymbol{\theta}_t^i)$, $\mathbf{F}(\boldsymbol{\theta}_t^i)$, $\mathbf{V}(\boldsymbol{\theta}_t^i)$, and $\boldsymbol{\partial}_{\bar{\mathbf{f}}(\mathbf{U}_t)}^{\mathrm{T}}\Sigma_{\mathbf{U}}\boldsymbol{\partial}_{\bar{\mathbf{f}}(\mathbf{U}_t)} + \sigma^2\mathbf{I}$, given the hyperparameters $\boldsymbol{\theta}_t^i$.
   c) Calculating $\mathbf{f}_{t|t-1}^{c,i}, \mathbf{P}_{t|t-1}^{c,i}$ according to the predict step of Kalman filter by using $\tilde{\mathbf{f}}_{t-1|t-1}^{c,i}, \tilde{\mathbf{P}}_{t-1|t-1}^{c,i}$.
   d) Calculating $\mathbf{f}_{t|t}^{c,i}, \mathbf{P}_{t|t}^{c,i}$ according to the update step of Kalman filter by using $\mathbf{f}_{t|t-1}^{c,i}, \mathbf{P}_{t|t-1}^{c,i}$.
   e) Calculating the importance weight $\bar{w}_t^i$ through (22) by using $\mathbf{f}_{t|t-1}^{c,i}, \mathbf{P}_{t|t-1}^{c,i}, \boldsymbol{\partial}_{\bar{\mathbf{f}}(\mathbf{U}_t)}^{\mathrm{T}}\Sigma_{\mathbf{U}}\boldsymbol{\partial}_{\bar{\mathbf{f}}(\mathbf{U}_t)} + \sigma^2\mathbf{I}$.
2) Normalizing the weight $w_t^i = \bar{w}_t^i / \Sigma_{j=1}^N \bar{w}_t^j$.
3) Estimating the hyperparameters and hidden function values based on weighted averaging

$$\hat{\boldsymbol{\theta}}_t = \Sigma_{i=1}^N w_t^i \boldsymbol{\theta}_t^i \tag{23}$$

$$\hat{\mathbf{f}}_{t|t}^c = \Sigma_{i=1}^N w_t^i \mathbf{f}_{t|t}^{c,i} \tag{24}$$

$$\hat{\mathbf{P}}_{t|t}^c = \Sigma_{i=1}^N w_t^i \Big(\mathbf{P}_{t|t}^{c,i} + \Big(\mathbf{f}_{t|t}^{c,i} - \hat{\mathbf{f}}_{t|t}^c\Big)\Big(\mathbf{f}_{t|t}^{c,i} - \hat{\mathbf{f}}_{t|t}^c\Big)^{\mathrm{T}}\Big) \tag{25}$$

such that the fingerprints in the updated radio map are

$$\hat{\mathbf{f}}_{t|t}^* = \mathbf{H}_t^*\hat{\mathbf{f}}_{t|t}^c \tag{26}$$

$$\hat{\mathbf{P}}^{*}_{t|t} = \mathbf{H}^{*}_{t}\hat{\mathbf{P}}^{c}_{t|t}\left(\mathbf{H}^{*}_{t}\right)^{\mathrm{T}} \tag{27}$$

where $\mathbf{H}^{*}_{t} = [\mathbf{0}, \mathbf{I}]$ is an index matrix to obtain the function value estimation at $\mathbf{X}_{*}$.

4) Resampling $\boldsymbol{\theta}^{i}_{t}, \mathbf{f}^{c,i}_{t|t}, \mathbf{P}^{c,i}_{t|t}$ with respect to the importance weight w^{i}_{t} to obtain $\tilde{\boldsymbol{\theta}}^{i}_{t}, \tilde{\mathbf{f}}^{c,i}_{t|t}, \tilde{\mathbf{P}}^{c,i}_{t|t}$ for the next step.
5) Increasing t by 1 and repeat step 1).

As depicted in Fig. 1, after a lightweight site survey is carried out at the beginning to collect a small amount of fingerprints, the standard GPS will be applied to build a coarse-grained radio map and the corresponding estimates of the hyperparameters will be assigned to $\boldsymbol{\theta}_0$ so as to launch MPEG. To be specific, the mean $\mathbb{E}(\mathbf{f}^{c}_{0})$ and variance $\mathbb{V}(\mathbf{f}^{c}_{0})$ at $\mathbf{U}^{c}_{0}$ are first evaluated according to (11) and (12); then, let $\tilde{\boldsymbol{\theta}}^{i}_{0} = \boldsymbol{\theta}_0$, $\tilde{\mathbf{P}}^{c,i}_{0|0} = \mathbb{V}(\mathbf{f}^{c}_{0})$, and draw $\tilde{\mathbf{f}}^{c,i}_{0|0}$ from $\mathcal{N}(\mathbb{E}(\mathbf{f}^{c}_{0}), \mathbb{V}(\mathbf{f}^{c}_{0}))$; consequently, MPEG can be started as long as the first set of crowdsourced fingerprints becomes available.

The major calculations of MPEG come from inverting matrices, e.g., $\mathbf{K}_t$ in (16), the computation complexity of which is $O(n^3)$ with n being the number of crowdsourced fingerprints, and therefore, the computation complexity of MPEG is $O(n^3N)$ with N being the number of particles.

From an information point of view, the more crowdsourced fingerprints are fed into MPEG, the more accurate radio map can be generated, which can be observed in the subsequent experiments. But a practical issue arises here to be when and how frequent MPEG should be scheduled. Considering the fact that indoor positioning services are usually provided in daytime, MPEG can thus be scheduled to run at midnight. As to the update frequency, two key factors, i.e., the amount of crowdsourced fingerprints and the environmental dynamics, must be taken into account. If the update frequency is too low, radio maps might become outdated, and meanwhile, too many crowdsourced fingerprints might be accumulated, such that running MPEG will cost a long time and even exhaust the memory of a computer. Otherwise, frequently updating radio maps may result in performance fluctuations due to insufficient crowdsourced fingerprints. Therefore, to tradeoff among various factors, radio maps are suggested to be updated no more than once a day and only if newly crowdsourced fingerprints cover or nearly cover their target spaces (which can be determined by localizing crowdsourced RSS measurements using the current radio map).

VI. Performance Evaluation

In this section, extensive experiments are conducted to thoroughly evaluate the performance of the proposed method.

A. Experimental Setup

In the experiments, realistic RSS measurements are collected in a big open space with a total area of nearly 1000 m^2, i.e., the reading room on the third floor of the library building in Inner Mongolia University, which includes 57 bookracks with the height of around 2 m as well as a number of desks and chairs, as illustrated in Fig. 3. The target space is divided by a regular lattice with the interval 1 m, such that totally 938 lattice points are selected as reference points.

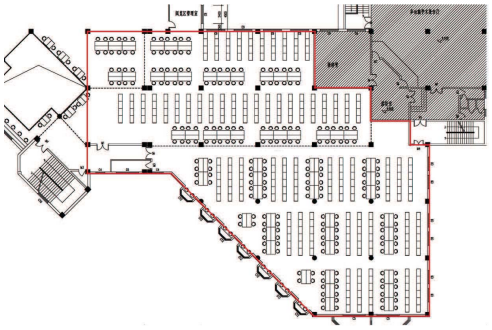

Fig. 3. Floor plan of the experimental space.

The experiments last for five months, and involve ten rounds of collecting RSS measurements at different times, e.g., weekday, weekend, holiday, daytime, and evening; see the caption in Fig. 7 for detailed informations. During each round, a male student with a smartphone (i.e., HUAWEI P7) held in front of his chest was asked to arbitrarily traverse the reading room as usual to produce training samples, and also walk along seven prespecified trajectories ranging between 20 and 30 m to produce testing samples; as a result, each round contains 700 to 1200 training samples which cover the whole target space. Besides, an Android APP was developed to trigger WiFi scan to collect RSS measurements from nearby APs and meanwhile record the inertial measurements from accelerometer and magnetometer for use in PDR at the frequencies of 1 and 100 Hz, respectively. It is noticeable that more than 100 distinct APs were detected in the target space, and most of them only provide occasional and extremely weak RSS measurements; hence, 22 APs with strongest RSS measurements were selected for use in the experiments.

Two GPR based approaches (i.e., ZeroM-GPR and LDM-GPR [20]), which build new radio maps using the crowdsourced training samples in each round, and a partial least squares regression (PLSR)-based approach were implemented for comparison. Note that PLSR was adopted in [23] to fuse crowdsourced RSS measurements with noisy location labels with radio maps, but it requests the smartphone to keep stationary at each crowdsourcing location for a period of time, which is obviously different from our scenario. Hence, in the experiments, PLSR just functions as a mathematical tool for fusing fingerprints with a radio map.

In order to validate the effectiveness of PDR, two versions of the proposed scheme, namely, MPEG-PDR and MPEG-LOC, were realized to include or exclude the PDR-based location calibration. Moreover, to guarantee the applicability of the mean function in (2), the target space was divided into ten small rectangular regions with the area of around 100 m^2, in each of which MPEG was performed with the particle number of 500. Correspondingly, the training samples were also divided into ten groups according to their location labels.

The experiments were realized in MATLAB using a Lenovo desktop computer with CPU i5-3470 and 16-GB RAM. The MLE problems for estimating hyperparameters in the GPR were solved using the MATLAB routine *fmincon*. The initial coarse-grained radio map was built using the training samples

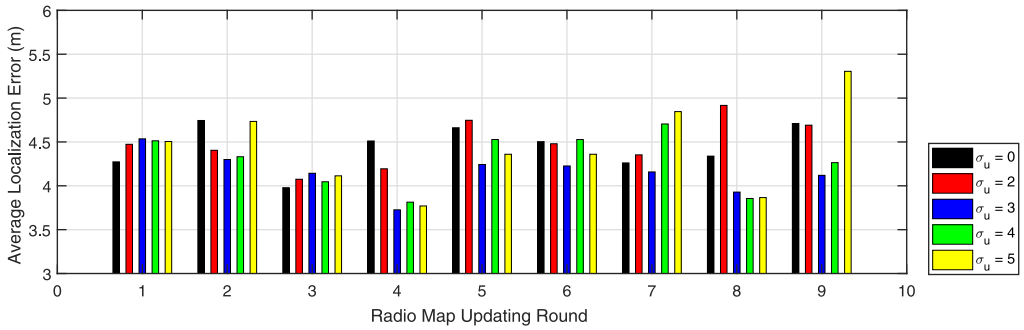

Fig. 4. Comparison of localization errors by using MPEG-LOC with respect to different σ_u.

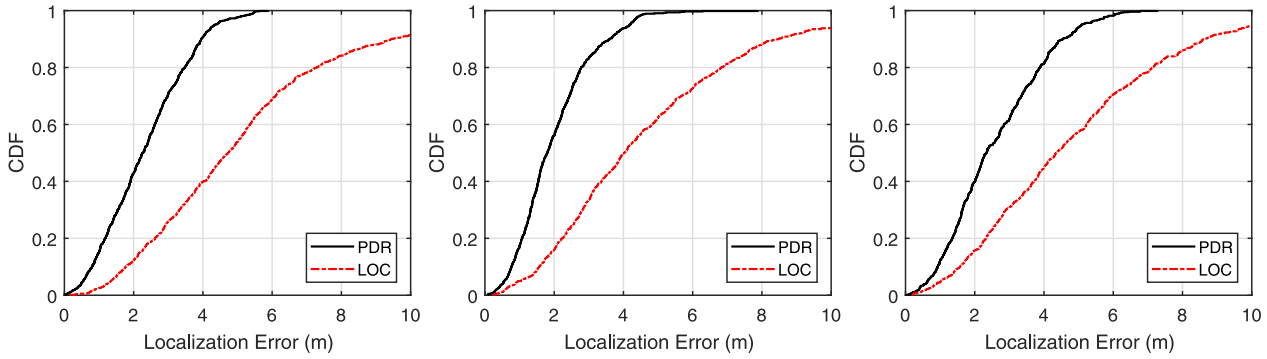

Fig. 5. Comparison of trajectory matching errors with/without PDR. (a) No. 2 Round(1 month). (b) No. 4 Round(1 month and 25 days). (c) No. 9 Round(5 months).

TABLE I
COMPARISON OF AVERAGE LOCALIZATION ERRORS BY USING MPEG-LOC WITH RESPECT TO DIFFERENT σ_u

σ_u	0	2	3	4	5
Average Localization Error (m)	4.44	4.48	4.15	4.29	4.43

obtained in the first round, and their accurate location labels were derived by manual configurations; then, the remaining nine sets of training samples were employed to produce nine rounds of radio map updates; accordingly, the testing samples in each round were used for performance comparison by using the weighted KNN (WKNN) method with $k = 6$.

B. Effectiveness of Extended GPR

It is evident that the extended GPR introduces the covariance matrix Σ_U in comparison with the standard GPR, and as such, we shall take into account different cases of Σ_U in order to evaluate the effectiveness of the extended GPR. For ease of treatments, Σ_U are assumed to be $\sigma_u^2\mathbf{I}$; that is to say, we can observe the impact of the extended GPR on localization through different values of σ_u, and particularly, when $\sigma_u = 0$, the extended GPR reduces to the standard GPR.

By changing the value of σ_u between 0 and 5, the resulting average localization errors in the 9 rounds of radio map updates by using the MPEG-LOC method are plotted in Fig. 4. As can be seen, different values of σ_u result in significantly different performance, but in most times, the extended GPR (i.e., $\sigma_u \neq 0$) is superior to the standard GPR (i.e., $\sigma_u = 0$).

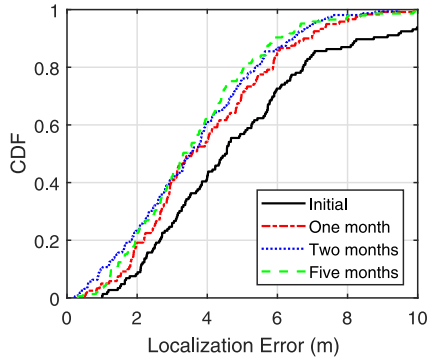

Fig. 6. Comparison of the localization errors produced by MPEG-LOC with respect to different times.

Moreover, the localization errors are averaged cross the nine rounds with respect to different σ_u, as listed in Table I. It reveals that the best localization accuracy can be achieved with $\sigma_u = 3$ and 4, which is consistent with the overall localization accuracy of the fingerprint-based IPS implemented in the experiments. Therefore, we let $\sigma_u = 3$ for MPEG-LOC and $\sigma_u = 2$ for MPEG-PDR in the following experiments.

C. Effectiveness of PDR

In order to validate the effectiveness of PDR, the trajectories in relation to testing RSS measurements in the No. 2, No. 4, and No. 9 rounds (i.e., corresponding to one month, nearly two months, and five months, respectively) are employed to evaluate the localization performance of simply using the

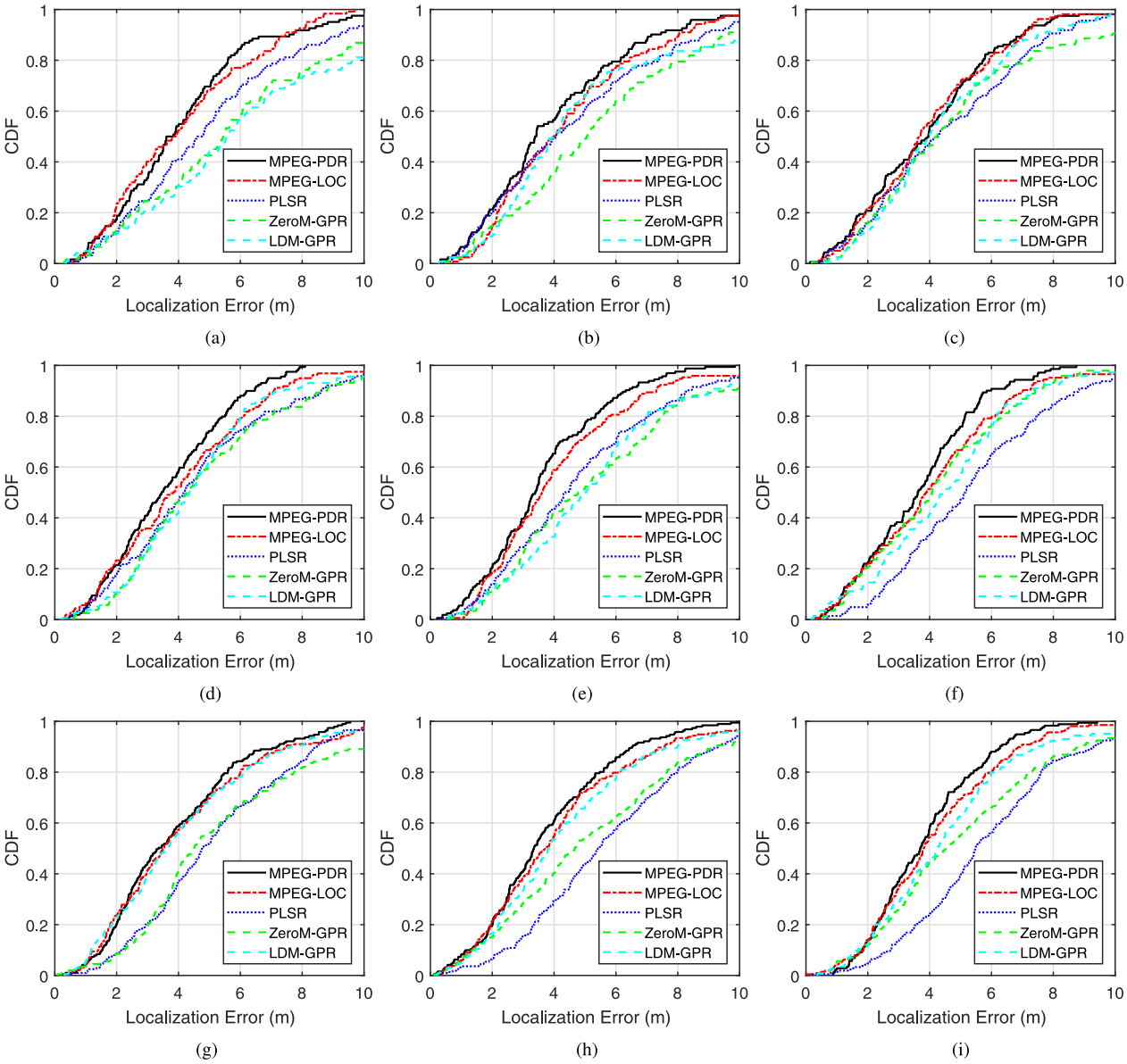

Fig. 7. Comparison of localization errors produced by different approaches at different times. (a) No. 1 Round (10 days). (b) No. 2 Round (1 month). (c) No. 3 Round (1 month and 7 days). (d) No. 4 Round (1 month and 25 days). (e) No. 5 Round (2 months and 18 days). (f) No. 6 Round (3 months and 15 days). (g) No. 7 Round (3 months and 25 days). (h) No. 8 Round (4 months and 5 days). (i) No. 9 Round (5 months).

TABLE II
COMPARISON OF LOCALIZATION ERRORS PRODUCED BY DIFFERENT APPROACHES

Method	Average Localization Error (m)										
	Initial	NO.1	NO.2	NO.3	NO.4	NO.5	NO.6	NO.7	NO.8	NO.9	Average
Original	4.98	4.70	4.96	5.14	5.44	5.89	5.06	5.67	6.88	6.48	5.58
MPEG-PDR	4.98	4.17	4.15	4.03	3.49	3.63	3.66	3.86	3.73	3.86	3.84
MPEG-LOC	4.98	4.53	4.30	4.14	3.72	4.24	4.23	4.16	3.93	4.12	4.16
PLSR	4.98	5.13	4.61	4.58	4.64	4.81	5.43	5.21	5.75	5.85	5.01
ZeroM-GPR	4.98	5.86	5.45	4.85	5.62	5.37	4.27	5.49	5.11	5.01	5.22
LDM-GPR	4.98	6.52	4.87	4.43	4.71	5.09	4.55	4.15	4.35	4.80	4.84

fingerprint-based IPS (with the legend of "LOC") and of combining the fingerprint-based IPS with PDR (with the legend of "PDR"), as illustrated in Fig. 5. It can be seen that the localization errors calibrated by PDR are almost always less than 8 m, whereas those by the fingerprint-based IPS can be as high as 14 m. Therefore, PDR significantly improves the trajectory matching accuracy, so as to provide accurate location labels for use in radio map updates with crowdsourced RSS measurements.

D. Effectiveness of Online Radio Map Update

Experiments are conducted to compare the IPS with and without online radio map update, namely MPEG-LOC and

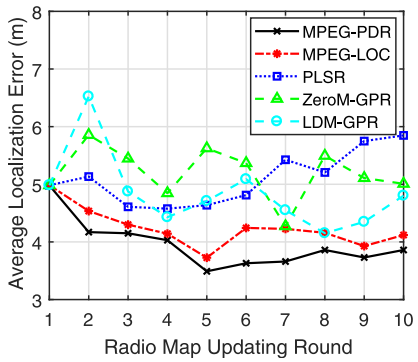

Fig. 8. Comparison of localization errors produced by different approaches with respect to nine rounds.

the original fingerprint-based IPS. As shown in Table II, with time going on, the average localization error of the original fingerprint-based IPS (termed "original") appears increase, but that of MPEG-LOC appears to be refined to some extent.

Moreover, the cumulative density function (CDF) of the localization errors produced by MPEG-LOC in three different rounds are plotted in Fig. 6. As can be seen, the localization errors of MPEG-LOC generally decrease with the radio map update. It can be concluded that recursively updating the radio map evidently benefits localization accuracy.

E. Comparison of Different Approaches

First of all, the CDFs of the localization errors produced by different approaches with respect to nine rounds of radio map updates are illustrated in Fig. 7. It can be found that, the proposed scheme, i.e., MPEG-PDR and MPEG-LOC, almost delivers better localization performance than the other three approaches in each round of radio map update, and in particular, MPEG-PDR produces the best localization accuracy.

Second, for ease of comparison, the average localization errors produced by the five different approaches are plotted in Fig. 8. As can be seen, during the nine rounds of radio map updates, the proposed scheme evidently provides more robust localization performance that its counterparts.

Third, the detailed average localization errors in each round and the total average values (over the nine rounds) are listed in Table II. As can be seen, the average localization error of MPEG-PDR decreases from 4.98 m in the beginning to 3.86 m after nine rounds of radio map updates, and meanwhile, that of MPEG-LOC decreases from 4.98 to 4.12 m; however, the other three approaches usually result in worse localization errors fluctuating around 5 m than the proposed scheme. Specifically, ZeroM-GPR derives worst localization performance, and PLSR outperforms ZeroM-GPR and LDM-GPR during the first several rounds, but appears to degrade after the No. 4 round. According to the average localization error over the nine rounds, it can be concluded that, in comparison with the original fingerprint-based IPS, MPEG-PDR, and MPEG-LOC are able to improve the localization accuracy by 31.2% and 25.4%, respectively, while the other three approaches can improve the localization accuracy by 13.3% at most.

However, particle filter and GPR involved in the proposed scheme result in a relatively high computation complexity. In the experiments, each round of updating the radio map costs around 14 min for MPEG-LOC and MPEG-PDR, around 2 min for ZeroM-GPR and LDM-GPR, and only around 2 s for PLSR. But, considering the fact the online radio map update can be scheduled at midnight, the relatively high computation complexity is still acceptable in practice.

In summary, the experiments confirm the effectiveness of the ideas adopted in the proposed scheme, i.e., extended GPR, recursive radio map update, and PDR-based location label calibration, in the sense that the performance of fingerprint-based IPSs are substantially improved; furthermore, the comparison among five different approaches validates the superiority and robustness of the proposed scheme.

VII. Conclusion

In this paper, we proposed to recursively update radio maps using crowdsourced fingerprints in an online fashion. To be specific, the standard GPR was extended to alleviate the influence of noisy location labels attached to crowdsourced RSS measurements; moreover, PDR was employed to further calibrate the noisy location labels in comparison with the traditional approach that relies on the original fingerprint-based IPS; on these grounds, MPEG was adopted to fuse crowdsourced fingerprints with existing radio map without the alignment of location labels. Extensive experiments were conducted, and a thorough comparison reveals that the proposed scheme outperforms the other three approaches in the literature in terms of both localization accuracy and robustness. This paper not only contributes to reducing the costs of building radio maps, but also makes it possible to update radio maps irrespective the amount of crowdsourced fingerprints.

For future works, we plan to implement the proposed scheme in a building-scale space by regularly crowdsourcing fingerprints with multiple participants and different smartphones.

References

[1] Z. Yuan *et al.*, "A pervasive integration platform of low-cost MEMS sensors and wireless signals for indoor localization," *IEEE Internet Things J.*, vol. 5, no. 6, pp. 4616–4631, Dec. 2018.

[2] X. Guo, N. Ansari, L. Li, and H. Li, "Indoor localization by fusing a group of fingerprints based on random forests," *IEEE Internet Things J.*, vol. 5, no. 6, pp. 4686–4698, Dec. 2018.

[3] M. Zhou, Y. Wang, Y. Liu, and Z. Tian, "An information-theoretic view of WLAN localization error bound in GPS-denied environment," *IEEE Trans. Veh. Technol.*, vol. 68, no. 4, pp. 4089–4093, Apr. 2019.

[4] P. Bahl and V. N. Padmanabhan, "RADAR: An in-building RF-based user location and tracking system," in *Proc. IEEE INFOCOM*, 2010, pp. 775–784.

[5] H. Zou, B. Huang, X. Lu, H. Jiang, and L. Xie, "A robust indoor positioning system based on the procrustes analysis and weighted extreme learning machine," *IEEE Trans. Wireless Commun.*, vol. 15, no. 2, pp. 1252–1266, Feb. 2016.

[6] B. Jia, B. Huang, H. Gao, and W. Li, "Dimension reduction in radio maps based on the supervised kernel principal component analysis," *Soft Comput.*, vol. 22, no. 23, pp. 7697–7703, Dec. 2018.

[7] M. Zhou, Y. Tang, Z. Tian, L. Xie, and W. Nie, "Robust neighborhood graphing for semi-supervised indoor localization with light-loaded location fingerprinting," *IEEE Internet Things J.*, vol. 5, no. 5, pp. 3378–3387, Oct. 2018.
[8] B. Jia, B. Huang, H. Gao, W. Li, and L. Hao, "Selecting critical WiFi APs for indoor localization based on a theoretical error analysis," *IEEE Access*, vol. 7, pp. 36312–36321, 2019.
[9] B. Ferris, D. Fox, and N. D. Lawrence, "WiFi-SLAM using Gaussian process latent variable models," in *Proc. IJCAI*, vol. 7, no. 1, 2007, pp. 2480–2485.
[10] A. Rai, K. K. Chintalapudi, V. N. Padmanabhan, and R. Sen, "Zee: Zero-effort crowdsourcing for indoor localization," in *Proc. Mobicom*, Istanbul, Turkey, 2012, pp. 293–304.
[11] Z. Yang, C. Wu, and Y. Liu, "Locating in fingerprint space: Wireless indoor localization with little human intervention," in *Proc. 18th Annu. Int. Conf. Mobile Comput. Netw.*, 2012, pp. 269–280.
[12] C. Wu, Z. Yang, Y. Liu, and W. Xi, "WILL: Wireless indoor localization without site survey," *IEEE Trans. Parallel Distrib. Syst.*, vol. 24, no. 4, pp. 839–848, Apr. 2013.
[13] R. W. Ouyang, A. K.-S. Wong, C.-T. Lea, and M. Chiang, "Indoor location estimation with reduced calibration exploiting unlabeled data via hybrid generative/discriminative learning," *IEEE Trans. Mobile Comput.*, vol. 11, no. 11, pp. 1613–1626, Nov. 2012.
[14] D. Sikeridis, B. P. Rimal, I. Papapanagiotou, and M. Devetsikiotis, "Unsupervised crowd-assisted learning enabling location-aware facilities," *IEEE Internet Things J.*, vol. 5, no. 6, pp. 4699–4713, Dec. 2018.
[15] S. Kumar, R. M. Hegde, and N. Trigoni, "Gaussian process regression for fingerprinting based localization," *Ad Hoc Netw.*, vol. 51, pp. 1–10, Nov. 2016.
[16] H. Zhao, B. Huang, and B. Jia, "Applying kriging interpolation for WiFi fingerprinting based indoor positioning systems," in *Proc. IEEE WCNC*, Doha, Qatar, 2016, pp. 1–6.
[17] K. Chang and D. Han, "Crowdsourcing-based radio map update automation for Wi-Fi positioning systems," in *Proc. 3rd ACM SIGSPATIAL Int. Workshop Crowdsourced Volunteered Geographic Inf.*, Dallas, TX, USA, 2014, pp. 24–31.
[18] S. He, W. Lin, and S.-H. G. Chan, "Indoor localization and automatic fingerprint update with altered ap signals," *IEEE Trans. Mobile Comput.*, vol. 16, no. 7, pp. 1897–1910, Jul. 2017.
[19] Z. Sun, Y. Chen, J. Qi, and J. Liu, "Adaptive localization through transfer learning in indoor Wi-Fi environment," in *Proc. IEEE ICMLA*, San Diego, CA, USA, 2008, pp. 331–336.
[20] M. M. Atia, A. Noureldin, and M. J. Korenberg, "Dynamic online-calibrated radio maps for indoor positioning in wireless local area networks," *IEEE Trans. Mobile Comput.*, vol. 12, no. 9, pp. 1774–1787, Sep. 2013.
[21] H. Zou, M. Jin, H. Jiang, L. Xie, and C. J. Spanos, "WinIPS: WiFi-based non-intrusive indoor positioning system with online radio map construction and adaptation," *IEEE Trans. Wireless Commun.*, vol. 16, no. 12, pp. 8118–8130, Dec. 2017.
[22] Y. Tao and L. Zhao, "A novel system for WiFi radio map automatic adaptation and indoor positioning," *IEEE Trans. Veh. Technol.*, vol. 67, no. 11, pp. 10683–10692, Nov. 2018.
[23] C. Wu, Z. Yang, and C. Xiao, "Automatic radio map adaptation for indoor localization using smartphones," *IEEE Trans. Mobile Comput.*, vol. 17, no. 3, pp. 517–528, Mar. 2018.
[24] B. Huang, G. Qi, X. Yang, L. Zhao, and H. Zou, "Exploiting cyclic features of walking for pedestrian dead reckoning with unconstrained smartphones," in *Proc. Ubicomp*, Heidelberg, Germany, 2016, pp. 374–385.
[25] A. McHutchon and C. E. Rasmussen, "Gaussian process training with input noise," in *Proc. Adv. Neural Inf. Process. Syst.*, Granada, Spain, 2011, pp. 1341–1349.
[26] Y. Wang and B. Chaib-Draa, "A marginalized particle Gaussian process regression," in *Advances in Neural Information Processing Systems 25*, F. Pereira, C. J. C. Burges, L. Bottou, and K. Q. Weinberger, Eds. Red Hook, NY, USA: Curran Assoc., 2012, pp. 1187–1195. [Online]. Available: http://papers.nips.cc/paper/4850-a-marginalized-particle-gaussian-process-regression.pdf
[27] Y. Ji, S. Biaz, S. Pandey, and P. Agrawal, "ARIADNE: A dynamic indoor signal map construction and localization system," in *Proc. MobiSys*, Uppsala, Sweden, 2006, pp. 151–164.
[28] K. Majeed, S. Sorour, T. Y. Al-Naffouri, and S. Valaee, "Indoor localization and radio map estimation using unsupervised manifold alignment with geometry perturbation," *IEEE Trans. Mobile Comput.*, vol. 15, no. 11, pp. 2794–2808, Nov. 2016.
[29] X. Yang and B. Huang, "An accurate step detection algorithm using unconstrained smartphones," in *Proc. IEEE CCDC*, Qingdao, China, 2015, pp. 5682–5687.
[30] H. Weinberg, "Using the ADXL202 in pedometer and personal navigation applications," Application Note AN-602, Analog Devices, Norwood, MA, USA, 2002.
[31] N. Kantas, A. Doucet, S. Singh, and J. M. Maciejowski, "An overview of sequential Monte carlo methods for parameter estimation in general state-space models," *IFAC Proc. Vol.*, vol. 42, no. 10, pp. 774–785, 2009.
[32] T. J. Page, Jr., "Multivariate statistics: A vector space approach," *J. Market. Res.*, vol. 21, no. 2, p. 236, 1984.

Baoqi Huang (S'08–M'12) received the Ph.D. degree in information engineering from Australian National University, Canberra, ACT, Australia, in 2012.

From 2013 to 2014, he was a Research Fellow with Nanyang Technological University, Singapore. He is with the College of Computer Science, Inner Mongolia University, Hohhot, China, where he is currently a Professor. His current research interests include wireless networks, sensor networks, mobile computing, and ubiquitous computing.

Dr. Huang was a recipient of the Chinese Government Award for Outstanding Chinese Students Abroad in 2011.

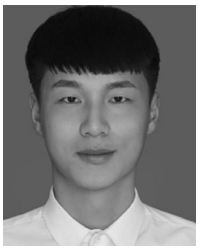

Zhendong Xu received the B.E. degree in computer science from Inner Mongolia University, Hohhot, China, in 2016, where he is currently pursuing the Ph.D. degree at the College of Computer Science.

His current research interests include mobile computing and ubiquitous computing.

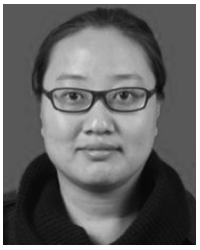

Bing Jia (M'16) received the Ph.D. degree from Jilin Univesity, Changchun, China, in 2013.

She is with the College of Computer Science, Inner Mongolia University, Hohhot, China, where she is currently an Associate Professor. Her current research interests include wireless networks, indoor localization, crowdsourcing, and mobile computing.

Guoqiang Mao (S'98–M'02–SM'08–F'18) was with the School of Electrical and Information Engineering, University of Sydney, Sydney, NSW, Australia. He joined the University of Technology Sydney, Ultimo, NSW, Australia, in 2014 as a Professor of wireless networking and the Director of the Center for Real-time Information Networks. He has authored or coauthored over 200 papers in international conferences and journals, which have been cited over 7000 times. His current research interests include intelligent transport systems, applied graph theory and its applications in telecommunications, Internet of Things, wireless sensor networks, wireless localization techniques and network modeling, and performance analysis.

Prof. Mao was a recipient of the Top Editor Award for outstanding contributions to the IEEE TRANSACTIONS ON VEHICULAR TECHNOLOGY in 2011, 2014, and 2015. He has been an Editor of the IEEE TRANSACTIONS ON INTELLIGENT TRANSPORTATION SYSTEMS since 2018, the IEEE TRANSACTIONS ON WIRELESS COMMUNICATIONS since 2014, and the IEEE TRANSACTIONS ON VEHICULAR TECHNOLOGY since 2010. He is the Co-Chair of the IEEE Intelligent Transport Systems Society Technical Committee on Communication Networks. He has served as the Chair, the Co-Chair, and a TPC member for a number of international conferences. He is a Fellow of IET.